OUR SUN. II. EARLY MASS LOSS OF 0.1 $M_\odot$ AND THE CASE OF THE MISSING LITHIUM

Arnold I. Boothroyd
Canadian Institute for Theoretical Astrophysics, University of Toronto
60 St. George Street, Toronto, Ontario, Canada M5S 1A1
and
I.-Juliana Sackmann and William A. Fowler
W. K. Kellogg Radiation Laboratory 106-38
California Institute of Technology, Pasadena, CA 91125, U. S. A.

ABSTRACT

We have computed detailed solar models, taking early–main-sequence mass loss into account. We have followed the nuclear destruction (and production) of ^{7}Li throughout the interior structure of the star during the entire evolution, keeping careful account of the changes in the surface lithium abundance due to mass loss and convection. We have considered initial masses of $M_i = 1.8\,M_\odot$, $1.5\,M_\odot$, $1.2\,M_\odot$, and $1.1\,M_\odot$, each with mass loss timescales of $\tau_m = 0.16$ Gyr, 0.5 Gyr, and 0.985 Gyr.

A solar model of initial mass $M_i \approx 1.1\,M_\odot$ *can solve the case of the missing solar lithium,* producing the observed surface lithium depletion of a factor of 100. Furthermore, this lithium depletion is *almost independent* of the mass loss timescale. With this mass loss of only $\Delta M \approx 0.1\,M_\odot$, there are only minor changes in the presolar helium abundance, the solar metallicity, the mixing length parameter, and the predicted solar neutrino capture rates. We estimate that this mass loss would cause the convective envelope to just reach the layers where ^{9}Be has been burned, resulting in little surface ^{9}Be depletion, in agreement with solar observations. The higher initial masses are ruled out unless there is some mechanism to *produce* ^{7}Li (and ^{9}Be) at the solar surface. Main-sequence mass loss reduces the required presolar helium abundance (which must always exceed the primordial abundance); this constrains the mass loss ΔM to be less than $0.7\,M_\odot$, $1.0\,M_\odot$, and $1.5-2\,M_\odot$ for mass loss timescales $\tau_m = 0.985$ Gyr, 0.5 Gyr, and 0.16 Gyr, respectively (a much weaker constraint than that obtained from ^{7}Li depletion).

For mass losing cases, ^{7}Li and ^{9}Be burning does *not* take place at usually assumed temperatures of $2.5 \times 10^6\,K$ and $3.3 \times 10^6\,K$, respectively, but requires higher *initial* temperatures of approximately $3 \times 10^6\,K$ and $4 \times 10^6\,K$, respectively. The difference is due to the decline of these temperatures caused by the mass loss. We have developed a simple prescription to estimate these initial temperatures for ^{7}Li and ^{9}Be burning in mass losing cases.

The luminosity history of our $M_i = 1.1\,M_\odot$ case is different from that of the standard sun, with an initial decline during the mass loss period (rather than a steady brightening), but with smaller total variation. This, together with the larger initial gravity and larger initial solar wind ($\dot{M}_i = [1-7] \times 10^{-10}\,M_\odot$/yr), would have had a significant effect on the solar planetary system, that should be explored further.

1. INTRODUCTION

It has been suggested by Willson, Bowen, & Struck-Marcell (1987) that stars of $\sim 1-2.5\,M_\odot$ may lose significant amounts of mass during early main-sequence evolution. They point out that it is just in this mass range that the extension of the Cepheid and RR Lyrae instability strip would intersect the main sequence, at spectral types from early A to mid F; they note that the pulsating δ Scuti stars lie in this range. Earlier, they have argued that

pulsation may drive most mass loss episodes during post–main-sequence evolution (Willson & Bowen 1984). They point out that pulsation on the main sequence might also drive mass loss, perhaps aided by the effects of relatively rapid rotation. Guzik, Willson, & Brunish (1987) applied such mass loss to the main-sequence evolution of a solar model, with initial mass $M_i = 2\ M_\odot$, and found that they could reproduce the present solar luminosity ($L_\odot$) and radius ($R_\odot$) at the solar age. Their mass loss exposed layers where the presolar lithium and beryllium had been completely destroyed: their models predicted an extreme overdepletion of these elements. This is in contrast to standard solar models, which predict *no* depletion during main-sequence evolution. On the other hand, the solar observations indicate a depletion by a factor of about 100 for ^{7}Li and little or no depletion of ^{9}Be (Boesgaard & Steigman 1985).

Swenson (1990) pointed out that, unless the initial mass is fairly large, standard models *do* exhibit some ^{7}Li depletion during pre–main-sequence contraction down the Hayashi track (Bodenheimer 1965), which should be taken into account. However, this pre–main-sequence ^{7}Li depletion is only by a factor of about two for standard models of solar mass and metallicity (Proffitt & Michaud 1989; Swenson, Stringfellow, & Faulkner 1990); higher-mass stars encounter even less pre–main-sequence ^{7}Li depletion. These standard models agree quite well with lithium abundance observations of Pleiades stars (age < 0.1 Gyr), although the relevant observations of Duncan & Jones (1983) at low effective temperatures have a fairly large scatter in lithium abundance compared (for example) to the observations of Hyades stars (age 0.6 Gyr) of Cayrel *et al.* (1984).

Pre–main-sequence ^{7}Li depletion *could* be significantly enhanced by some "non-standard" assumptions, such as strong overshooting below the formal boundary of envelope convection (D'Antona & Mazzitelli 1984; Kızıloğlu & Eryurt-Ezer 1985). Swenson *et al.* (1990) show that a not unreasonable enhancement in the contribution of metals to the interior opacities can result in greatly increased pre–main-sequence ^{7}Li depletion, perhaps even allowing one to match the ^{7}Li depletion of Hyades stars without requiring any further main-sequence ^{7}Li depletion. They did not "recalibrate" the helium abundance Y and mixing length parameter α again to the current sun *after* changing their opacities, but Swenson (1990) notes that even a large change in the *interior* opacities results in only a very small change in α. Thus Fig. 2 of Swenson *et al.* (1990) can be used to estimate the effect of changing the interior opacities on the pre–main-sequence ^{7}Li depletion of a model whose effective temperature is constrained: their 40% increase in the contribution of metals to the interior opacities (which they require to match the Hyades) results in slightly more than a factor of 10 increase in the amount of ^{7}Li depletion for such a model. Thus Hyades observations suggest an absolute upper limit of a factor of about 20 even for "non-standard" pre–main-sequence ^{7}Li depletion of a *solar* model, while Pleiades observations are consistent with the factor of two ^{7}Li depletion of a standard pre–main-sequence solar model. Lithium abundance observations of stars in a number of open clusters (see, e.g., Hobbs & Pilachowski 1988) suggest that most ^{7}Li depletion takes place on the main sequence for stars of 1 $M_\odot$ and above: the amount of depletion tends to increase (for fixed stellar mass) with increasing cluster age, at least up to an age of ~ 5 Gyr. We will assume that pre–main-sequence solar ^{7}Li depletion was relatively slight.

Clearly, depending on one's choice of mass loss, one can produce any amount of *main-sequence* ^{7}Li depletion: no mass loss (a standard solar model) results in no depletion, while a mass loss of $\Delta M = 1.0\ M_\odot$ results in total depletion. It was our intent to explore the consequences of different amounts of mass loss, and of different mass loss timescales. We wished to determine just how much mass loss was necessary to account for the observed solar ^{7}Li depletion. Throughout this work, we assume that no other mechanism (such as diffusion, meridional circulation, rotation-induced turbulent mixing, convective overshoot, or variable mixing length) acts to deplete surface lithium.

Guzik *et al.* (1987) also showed that their solar models with mass loss of $\Delta M = 1.0\ M_\odot$ required a presolar helium abundance Y lower by 0.04 than their standard model. We wished to explore further this reduction in the presolar helium abundance. Specifically, we wished to obtain an upper limit on the mass loss, determined by the requirement that the presolar helium content must always be larger than the primordial Big Bang value. This is a completely independent constraint on the mass loss from that obtained from the ^{7}Li depletion. We have taken the primordial Big Bang helium abundance to be $Y_p = 0.239 \pm 0.015$, as obtained by observations of

galactic and extragalactic H II regions (Boesgaard & Steigman 1985). Galactic chemical evolution would increase the expected presolar helium abundance: Maeder (1984) estimated this enrichment as $1 \lesssim \Delta Y/\Delta Z \lesssim 2.3$, which would yield a presolar helium enrichment of $0.015 \lesssim \Delta Y \lesssim 0.05$ (given the solar metallicity of $Z \approx 0.02$). Guzik *et al.* (1987) obtained a presolar helium abundance of $Y = 0.24$ for their standard solar model: this is a very low value, equal to the primordial helium abundance. They obtained such a low value due to their use of the older Cox & Stewart (1970) opacity tables. Guenther, Jaffe, & Demarque (1989) showed conclusively that the presolar helium abundance obtained from a standard solar model depends sensitively on the opacities used: in their models, use of the older Cox & Stewart (1970) opacity tables yielded $Y = 0.24$, while the more recent opacities from the Los Alamos Opacity Library (LAOL) yielded $Y = 0.28$. In order to use the presolar helium abundance as a constraint on main-sequence mass loss, it is imperative to use the best available opacity data.

Recently, Brown *et al.* (1990) have placed a direct observational limit on main-sequence mass loss. VLA radio continuum observations of 17 A and F dwarfs placed upper limits of $\sim 10^{-9}\ M_\odot$/yr on the mass loss rates (for *ionized* material), with a few upper limits as low as $10^{-10}\ M_\odot$/yr. Most of the 17 observed stars have large rotational velocities and are known or suspected pulsating stars; some are members of the Ursa Major cluster (age ~ 0.3 Gyr). From these results, it seems improbable that main-sequence mass loss of $\Delta M = 1.0\,M_\odot$ could occur in any significant fraction of such stars, but mass loss of up to several tenths of a solar mass is not ruled out.

We used the most up-to-date opacity data (including some molecular opacities) and nuclear reaction rates, and performed detailed evolutionary runs with various amounts and timescales for main-sequence mass loss. We computed several standard solar models without mass loss (see Sackmann, Boothroyd, & Fowler 1990: hereafter Paper I); these models were in excellent agreement with recent standard solar models of other authors. Our presolar helium abundance for these standard solar models was $Y = 0.28$.

Hobbs, Iben, & Pilachowski (1989) recently presented a simple analytic formula to obtain the mass loss associated with a given lithium depletion: the surface lithium abundance drops exponentially with the amount of mass lost, after the base of the convective envelope reaches the point where lithium has been burned. (In a note added in proof, the above authors mentioned that this approach had already been independently developed by Weymann & Sears [1965].) The attractiveness of their formula is that the mass loss can be computed as soon as one knows (i) the mass of the convective envelope, (ii) the depth (in mass) below which lithium is burned, and (iii) the observed lithium depletion. The above masses can be estimated from constant-mass models, available in the literature. We wished to compare the predictions of this analytic formula with results obtained from detailed mass-losing, lithium-burning evolutionary models; this would provide guidance as to the best choice for the two mass parameters on which the analytic formula depends. Swenson (1990), in collaboration with Faulkner, has found recently that in fact this formula is overly simple and can give misleading results; we point out some possible pitfalls in our discussion (§ 3.7.2).

We describe our methods in § 2, and discuss our results in § 3. Our key results are summarized in § 4.

2. METHODS

Our stellar evolutionary code is described in some detail in Boothroyd & Sackmann (1988), with some modifications as described in Paper I. Our nuclear reaction rates are those of Caughlan & Fowler (1988). We followed ^{3}He and ^{7}Li abundances explicitly throughout the star, although non-equilibrium *energy generation* contributions were ignored. We included explicitly the *destruction* of ^{7}Li via the $^7\mathrm{Li}(p,\alpha)^4\mathrm{He}$ reaction, and ^{7}Li *production* via the *p-p* chain: we included not only the basic *p-p* reaction rate (which governs ^{3}He production), but also the burning rates for ^{3}He via the $^3\mathrm{He}(^3\mathrm{He},2p)^4\mathrm{He}$ and $^3\mathrm{He}(\alpha,\gamma)^7\mathrm{Be}$ reactions, as well as the temperature dependence of the branching ratio between the $^7\mathrm{Be}(e^-,\nu\gamma)^7\mathrm{Li}$ and $^7\mathrm{Be}(p,\gamma)^8\mathrm{B}$ reactions. (Note that, for purposes of observable surface ^{7}Li depletion, ^{7}Li production is unimportant: it results in interior equilibrium abundances Li/H $< 10^{-15}$, far below the detection threshold.)

Our opacities were those of LAOL, which included the opacities of some molecules (Keady 1985). Neutrino absorption cross sections were taken from Bahcall & Ulrich (1988), as in Paper I.

2.1. *Mass Loss and Surface Lithium Depletion*

We considered an exponentially decreasing solar mass as a function of time on the early main sequence. We chose to decay exponentially towards $0.99\,M_\odot$, and cut off the mass loss when the mass reached $1.0\,M_\odot$, in order that our solar model should have a mass of exactly $1.0\,M_\odot$ at the solar age. Thus the solar mass $M(t)$ was given by

$$M(t) = \begin{cases} 0.99\,M_\odot + (M_i - 0.99\,M_\odot)e^{-t/\tau_m}\,, & \text{for } t \text{ such that } M(t) > 1.0\,M_\odot \\ 1.0\,M_\odot\,, & \text{otherwise} \end{cases} \tag{1}$$

where M_i is the initial mass and τ_m is the timescale for mass loss. This implies a mass loss rate of

$$\dot{M}(t) = \begin{cases} -\dfrac{(M_i - 0.99\,M_\odot)}{\tau_m} e^{-t/\tau_m}\,, & M(t) > 1.0\,M_\odot \\ 0\,, & \text{otherwise} \end{cases} \tag{2}$$

For initial masses M_i we used $1.0\,M_\odot$, $1.1\,M_\odot$, $1.2\,M_\odot$, $1.5\,M_\odot$, and $1.8\,M_\odot$. At the start, we also considered $M_i = 2.0\,M_\odot$, because Willson, Guzik, & Brunish (1986) had used this initial mass, but eliminated this case because even the $M_i = 1.8\,M_\odot$ case turned out to be rather extreme. For mass loss timescales τ_m, we used 0.16 Gyr, 0.5 Gyr, and 0.985 Gyr. We chose the value of $\tau_m = 0.16$ Gyr to match the smaller of the values used by Willson *et al.* (1986), which was the only solar mass loss paper available to us when we started our work. The value of $\tau_m = 0.985$ Gyr was chosen as the largest timescale which would reduce an initial mass of $2.0\,M_\odot$ down to $1.0\,M_\odot$ by the solar age, when using the mass loss formula of eqs. (1) and (2). The value of $\tau_m = 0.5$ Gyr was chosen as an intermediate value. For the $M_i = 1.1\,M_\odot$ cases, the *initial* mass loss rates are $\dot{M}_i = 6.9 \times 10^{-10}\,M_\odot$/yr, $2.2 \times 10^{-10}\,M_\odot$/yr, and $1.1 \times 10^{-10}\,M_\odot$/yr for the short, intermediate, and long timescales, respectively. For the $M_i = 1.8\,M_\odot$ cases, the corresponding initial mass loss rates are $\dot{M}_i = 5.1 \times 10^{-9}\,M_\odot$/yr, $1.6 \times 10^{-9}\,M_\odot$/yr, and $8.2 \times 10^{-10}\,M_\odot$/yr, respectively (these are pushing the A and F dwarf mass loss limits of $\lesssim 10^{-9}\,M_\odot$/yr found by Brown *et al.* [1990]).

Our program handled mass loss by removing a small amount of mass from the surface of the static envelope at each timestep; a number of constraints on the size of the timestep ensured that not more than $10^{-3}\,M_\odot$ were removed per timestep, and usually somewhat less. Even a mass of $10^{-3}\,M_\odot$ could be large (or at least significant) compared to the mass of the convective envelope, which serves as a reservoir for presolar lithium. Thus it is necessary to exercise particular care in following the surface abundance of lithium, to avoid overestimating the depletion. For a convective envelope of mass M_{ce} (with lithium abundance Li_e) losing matter at the surface and engulfing lithium-depleted matter (lithium abundance Li_b) at its base, the lithium abundance changes according to

$$\frac{d\mathrm{Li}_e}{dM} = -\frac{(\mathrm{Li}_b - \mathrm{Li}_e)}{M_{ce}}\,. \tag{3}$$

During periods when $\mathrm{Li}_b \approx 0$, this results in $\mathrm{Li}_e \propto \exp(-\Delta M/M_{ce})$, where ΔM is the amount of mass loss: this leads to the lithium formulas of Weymann & Sears (1965) and of Hobbs *et al.* (1989). However, in general Li_b is not zero, nor is it even necessarily constant: the strong temperature dependence of the $^7\mathrm{Li}(p,\alpha)^4\mathrm{He}$ reaction means that the lithium abundance could be significantly different from one mass layer to the next in the region where it was only partially destroyed. It is a good approximation to say that the interior lithium abundance Li_b drops exponentially with mass between its values $\mathrm{Li}_b^{(k)}$ at mass layer M_k and $\mathrm{Li}_b^{(k-1)}$ at mass layer M_{k-1} further in, particularly if the mass layers are close enough together that these two lithium abundances are not too different. It is also a good approximation to say that the mass of the convective envelope is constant over a timestep. Under these assumptions, if the envelope lithium abundance has a value $\mathrm{Li}_e^{(k)}$ when the base of the convective envelope reaches the mass

layer M_k, then after mass loss has caused the base of the convective envelope to reach down to the layer M_{k-1} below, the envelope lithium abundance will be

$$\mathrm{Li}_e^{(k-1)} = \left[\mathrm{Li}_e^{(k)} - \frac{\mathrm{Li}_b^{(k)}}{1-\lambda M_{ce}}\right] e^{-(M_k - M_{k-1})/M_{ce}} + \frac{\mathrm{Li}_b^{(k-1)}}{1-\lambda M_{ce}}\,, \qquad \text{where} \quad \lambda \equiv \frac{\ln\left(\mathrm{Li}_b^{(k)}/\mathrm{Li}_b^{(k-1)}\right)}{M_k - M_{k-1}}\,. \tag{4}$$

This solution of eq. (3) applies except in the (improbable) case that $\lambda M_{ce} = 1$, in which case one finds $\mathrm{Li}_e^{(k-1)} = \mathrm{Li}_e^{(k)} e^{-(M_k - M_{k-1})/M_{ce}} + [(M_k - M_{k-1})/M_{ce}]\mathrm{Li}_b^{(k-1)}$. (Of course, if there is no convective envelope, i.e., $M_{ce} = 0$, then the surface lithium abundance is simply that of the mass layer that has been exposed by mass loss.) The above equations were applied when removing mass at each timestep.

2.2. *Presolar Abundances*

For the ZAMS ^{7}Li abundance, we took a number ratio of Li/H $= 1.0 \times 10^{-9}$, the value inferred for the abundance in the interstellar medium by Boesgaard & Steigman (1985), using the uniformity of the maximum observed abundances in main-sequence Pop I stars, both field stars and open galactic clusters. (Both Proffitt & Michaud [1989] and Swenson *et al.* [1990] assume a slightly higher initial ^{7}Li abundance, which is then depleted slightly during pre–main-sequence evolution, ending up near Li/H $= 1.0 \times 10^{-9}$ by the ZAMS for stars of mass $1.0\,M_\odot$ and up.) For presolar ^{3}He, we assumed that deuterium had already burned to ^{3}He, and took a number ratio of $^3\mathrm{He}/^4\mathrm{He} = 4.0 \times 10^{-4}$ (Boesgaard & Steigman 1985). As in Paper I, the solar metal abundance was obtained from the recent Grevesse (1984) value of the mass ratio $Z/X = 0.02766$; presolar C, N, and O abundances were also those of Grevesse (1984). The initial CNO isotopic ratios were selected according to the observed solar system number ratios, namely $^{12}\mathrm{C}/^{13}\mathrm{C} = 90$ and $^{16}\mathrm{O}/^{17}\mathrm{O} = 2660$ (Dominy & Wallerstein 1987) and $^{16}\mathrm{O}/^{18}\mathrm{O} = 500$ (Dominy, Wallerstein, & Suntzeff 1986).

2.3. *The Present Sun*

For the present solar luminosity, we used a value of $L_\odot = 3.90 \times 10^{33}$ erg/sec (Allen 1963). This is 1% higher than the more recent value given by Bahcall *et al.* (1982), but this will not have a significant effect on our results (see discussion in Paper I). With a solar radius of $R_\odot = 6.96 \times 10^{10}$ cm (Allen 1963), one obtains an effective temperature of $\log T_e = 3.7623$. We used a time interval of 4.55 Gyr from our homogeneous initial model to the present sun; for a $1.0\,M_\odot$ standard solar model, the time from the initial homogeneous model to the zero age main sequence (ZAMS) was about 12 million years, so that our solar age was about 4.54 Gyr (see discussion in Paper I).

Our initial models were chemically homogeneous models in hydrostatic equilibrium, supported by nuclear burning alone (no contraction). These soon converge to the correct pre–main-sequence evolution, as may be seen by comparing the tracks of our models in the H-R Diagram (see Fig. 1: note that our mass loss rates were too small to have much effect on pre–main-sequence evolution) with the full pre–main-sequence tracks presented by Proffitt & Michaud (1989). However, any pre–main-sequence ^{7}Li depletion would take place *prior* to the starting points for our models.

For any initial mass M_i and mass loss timescale τ_m, we selected trial values of the presolar helium abundance Y and the mixing length parameter α (with Z obtained from the Grevesse [1984] Z/X ratio), and evolved this model up to the solar age. Several such trial evolutions allowed us to zero in on the appropriate values for Y and α in order to match the solar luminosity and effective temperature at the solar age. For the $M_i = 1.2\,M_\odot$, $1.5\,M_\odot$, and $1.8\,M_\odot$ cases (which were not of prime interest to us, as discussed in § 3), we matched these values to within 0.2%; on the other hand, for the $M_i = 1.1\,M_\odot$ case and the standard solar model we matched to 0.05%.

2.4. *Other Details of the Models*

Our models had about 250 mass layers in the interior (i.e., $\log T \geq 6.3$, which comprises about 98% of the solar mass); the surrounding static envelope had about 350 mass layers below the photosphere and 200 in the gray

atmosphere above it. The standard solar model (without mass loss) required about 130 timesteps to reach the present sun, with the longest timestep being 125 million years. Timesteps were considerably shorter during the periods of mass loss; the $M_i = 1.1\,M_\odot$ case required about 240 timesteps to reach the present sun, while the $M_i = 1.8\,M_\odot$ required about 1400 timesteps.

The models presented in this paper include pressure ionization effects in the static envelope; as discussed in Paper I, this is of minor importance. The main difference was that the inclusion of pressure ionization required a 10% larger value of the mixing length parameter α to match the solar effective temperature; note that this increase in the mixing length to compensate the change in the equation of state did *not* drive the convective envelope deeper, nor raise the temperature significantly at the base of the convective envelope.

3. RESULTS AND DISCUSSION

The basic characteristics of our solar models are presented in Table 1; note that for the mass-losing models to reproduce the solar characteristics at the solar age required significantly different chemical compositions.

3.1. *The H-R Diagram*

Fig. 1*a* shows how mass loss on the early main sequence affects the evolution of a star in the H-R Diagram (up to the solar age), for the $M_i = 1.8\,M_\odot$, $1.5\,M_\odot$, $1.2\,M_\odot$, and $1.1\,M_\odot$ cases, with mass loss timescale $\tau_m = 0.16\,\mathrm{Gyr}$; for comparison, the evolution of a standard solar model (up to the red giant branch) is also shown. The loops to the red of the zero age main sequence (ZAMS) are not a consequence of the mass loss: rather, they are part of the rapid pre–main-sequence evolution from a chemically homogeneous model to the appropriate nuclear equilibrium at the star's center. The first short downward stretch corresponds to ^{13}C approaching equilibrium with ^{12}C. (Note that even the $M_i = 1.0\,M_\odot$ standard solar model encounters this stage, but it is superimposed on the early main-sequence track in the H-R Diagram. If the full pre–main-sequence evolution had been followed, ^{13}C burning would have started slightly earlier, but this would not make very much difference.) The next longer upward stretch (taking 5 to 10 million years for the $1.8\,M_\odot$ and $1.5\,M_\odot$ cases) corresponds to ^{12}C (and ^{13}C) approaching equilibrium with ^{14}N; for the cases of $M_i \leq 1.2\,M_\odot$, this latter equilibrium is not reached for 40 to 200 million years, well into the main sequence. To define the ZAMS is not trivial, particularly for the mass losing cases. For a constant-mass case, post-ZAMS evolution is *upward* from the ZAMS; for a mass-losing case, post-ZAMS evolution is *downward*, approximately *along* the ZAMS of stars of lower mass. We chose to define the ZAMS at the point which we would have chosen for a constant-mass case of the same mass and composition, as shown in Fig. 1. Note, however, that mass loss always started at our initial, chemically homogeneous model.

Figs. 1*b*, *c*, and *d* show an expanded view of the approach in the H-R Diagram of the mass-losing cases to the $1.0\,M_\odot$ case, for each of the mass loss timescales τ_m. Let us ignore the pre–main-sequence evolution. The mass losing cases move down the main sequence until mass loss terminates; at this point they intercept the position in the H-R Diagram of the $1.0\,M_\odot$ (constant-mass) case at the corresponding time. For a short mass loss timescale, the mass-losing cases intercept the $1.0\,M_\odot$ track earlier in its evolution than for a long mass loss timescale. After mass loss terminates, all models follow the same path towards the present sun.

3.2. *The Luminosity History*

Figs. 2*a*, *b*, and *c* illustrate the history of the luminosity (up to the present) of our mass-losing solar models, as compared to the standard case. The cases with high initial masses naturally start out with initial luminosities very much larger than that of the present sun, as much as a factor of 10 for the $M_i = 1.8\,M_\odot$ case; note however that the $M_i = 1.1\,M_\odot$ case starts out with a luminosity only very slightly higher than that of the present sun, or about 50% brighter than the initial standard (constant-mass) case. Thus the $M_i = 1.1\,M_\odot$ cases encounter less luminosity change between the ZAMS and the present than does the standard case, particularly for long mass loss timescales.

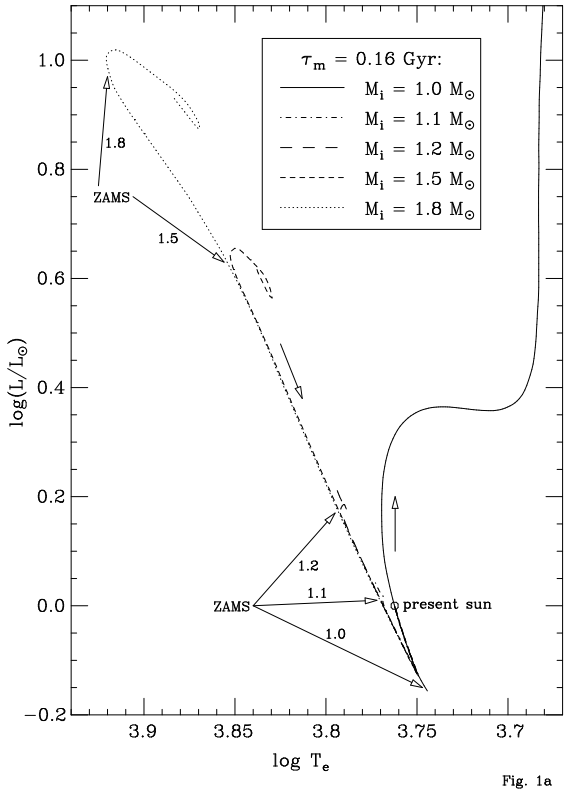

Fig. 1a

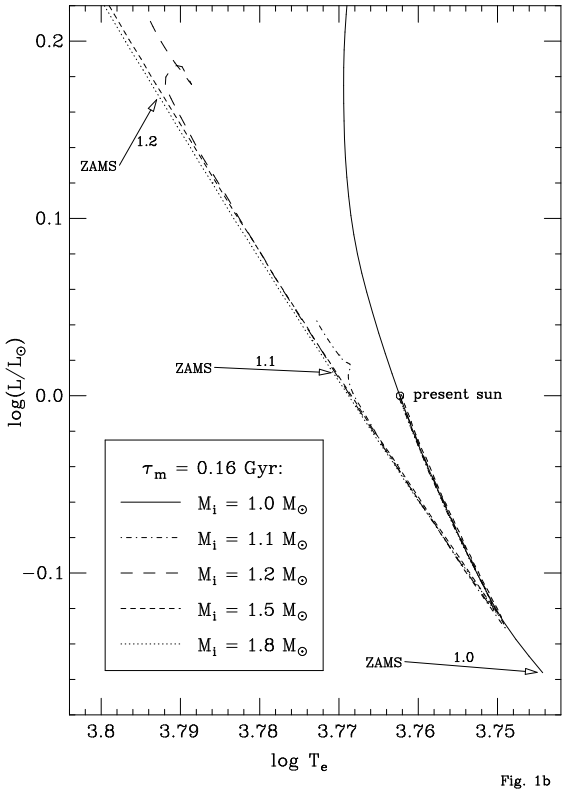

Fig. 1b

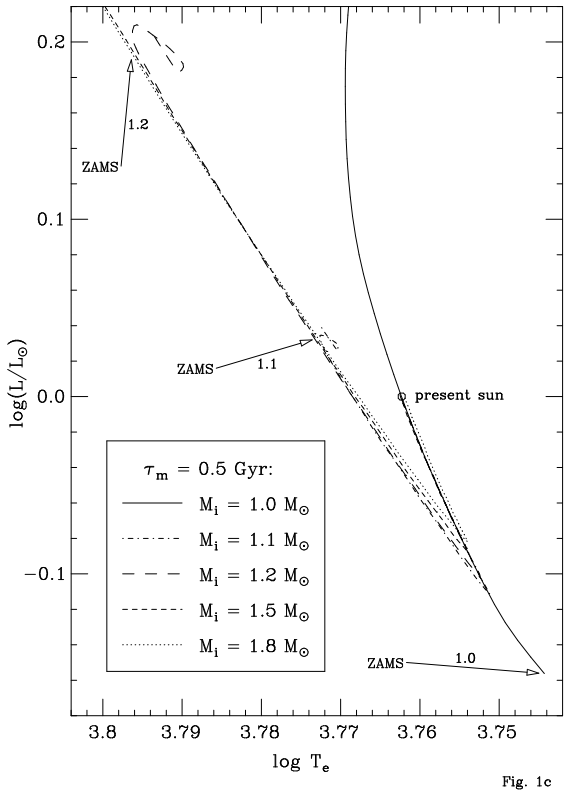

Fig. 1c

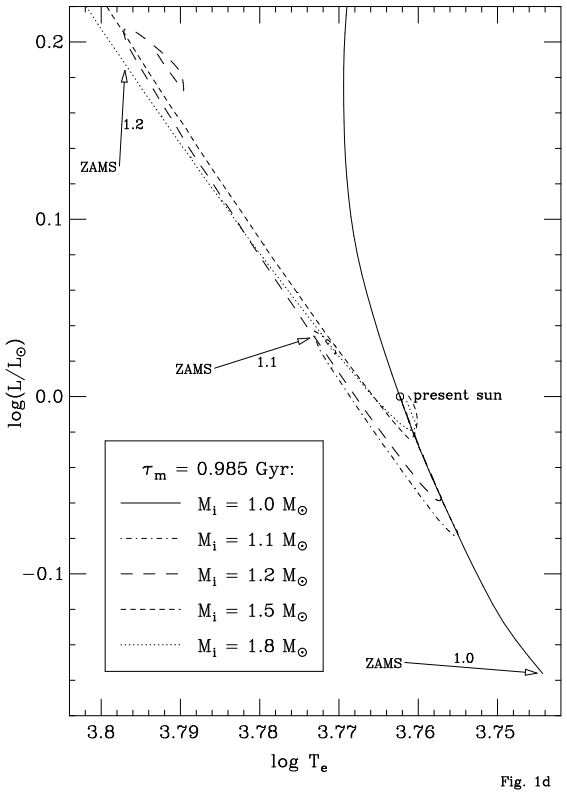

Fig. 1d

Fig. 1—The Hertzsprung-Russell Diagram for mass loss on the early main sequence; for comparison, the evolution of the Standard Sun is also shown.

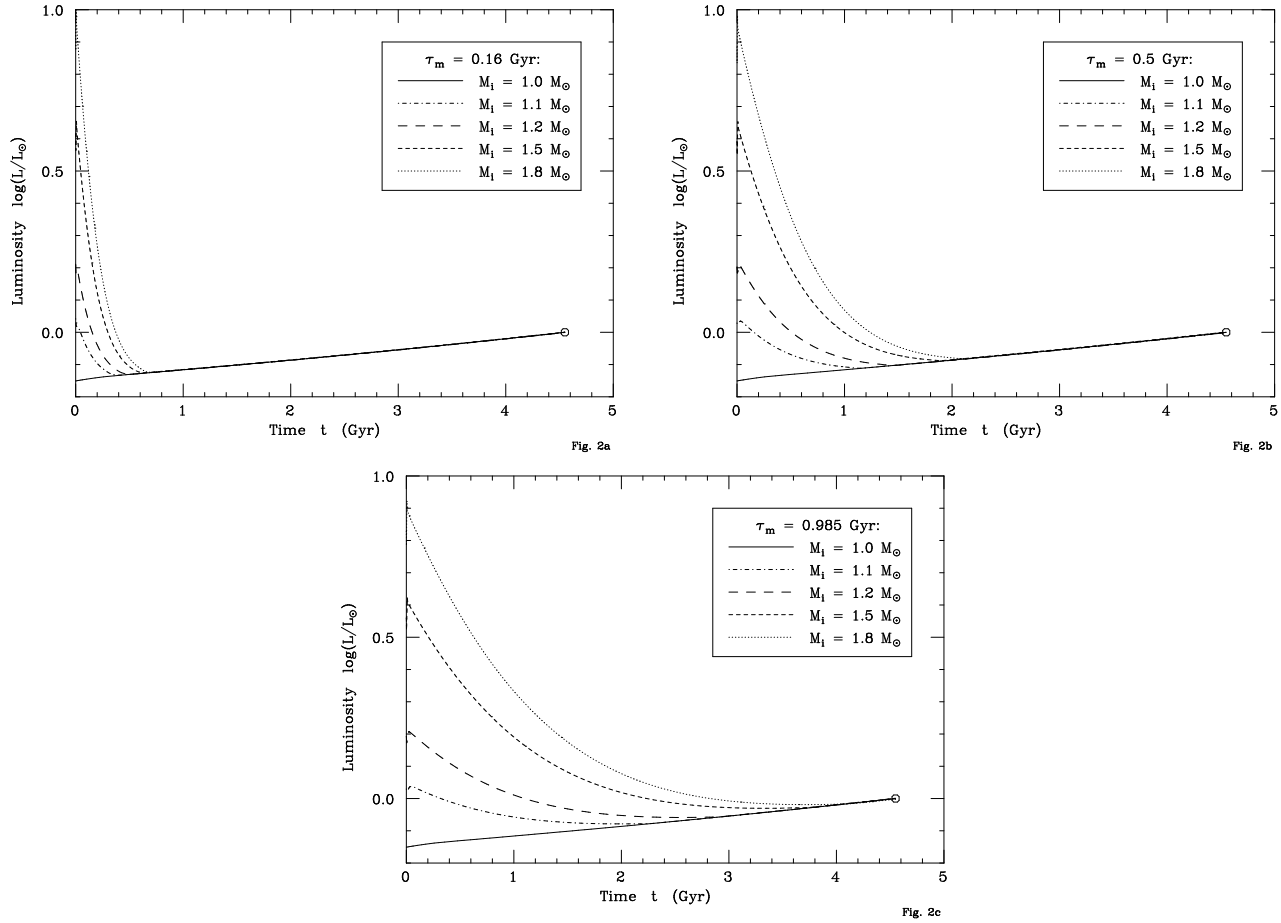

Fig. 2—The luminosity history on the main sequence for mass losing cases and the Standard Sun.

This different history of the luminosity and gravitational attraction of the sun, together with the much larger solar wind, could have a significant impact on the solar system.

3.3. *The Presolar Helium Abundance*

Fig. 3 illustrates how mass loss reduces the required presolar helium content Y. For the short mass loss timescale ($\tau_m = 0.16\,\mathrm{Gyr}$), the presolar value of Y remains nearly constant for different values of the initial mass M_i. However, for the longer mass loss timescales, there is a *large* reduction in the presolar Y for the larger initial masses: for $M_i = 1.8\,M_\odot$ with $\tau_m = 0.5\,\mathrm{Gyr}$, the presolar Y is reduced by 0.03, namely to $Y = 0.25$ (from $Y = 0.28$ for the standard model); for $M_i = 1.8\,M_\odot$ with $\tau_m = 0.985\,\mathrm{Gyr}$ (our longest timescale case), the presolar Y is reduced by nearly 0.06, to $Y = 0.224$.

The reason for this behavior of Y as a function of M_i and τ_m is clear. If the mass loss timescale τ_m is short, even a large initial mass M_i is reduced very quickly to $1.0\,M_\odot$, and the interior abundance profile is still very similar to that of the standard (constant-mass) case at the same age. However, if the mass loss timescale is long and the initial mass is large, the star remains at a higher mass for a long time, and appreciable differences in the interior abundance profile have time to develop. These result in relatively large changes in the stellar structure at the solar age, requiring relatively large changes in the presolar helium abundance Y in order to match the observed solar luminosity.

Note the primordial helium abundance is $Y_p = 0.239 \pm 0.015$ (Boesgaard & Steigman 1985), while galactic chemical evolution will produce a helium enrichment ΔY probably between 0.015 and 0.05, as discussed in the

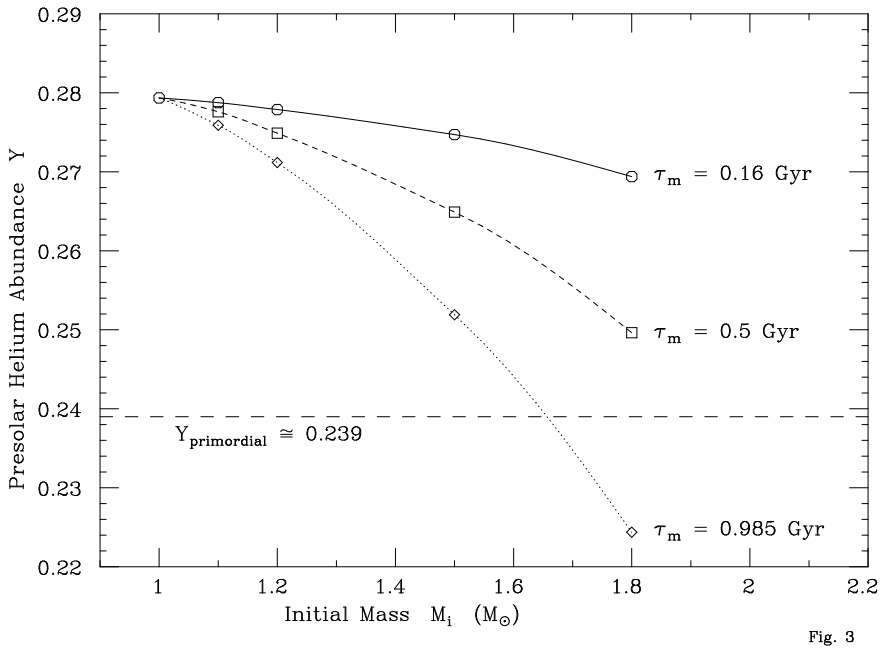

Fig. 3—The presolar helium abundance Y required for mass losing solar models, of various initial masses and mass loss timescales.

Introduction. Even taking the lower bound on each of these values, namely $Y_p = 0.239 - 0.015 = 0.224$ and $\Delta Y = 0.015$, the minimum possible presolar helium content can hardly fall below the sum of these, namely $Y \approx 0.24$. Thus the $M_i = 1.8\,M_\odot$ case with $\tau_m = 0.985$ Gyr, which has a presolar $Y = 0.224$, is not allowed. The requirement that the presolar helium abundance Y cannot fall below a value of 0.24 allows us to place an upper limit on the total amount of main-sequence mass loss:

$$\begin{aligned} M_i &\lesssim 1.7\,M_\odot \qquad \text{for} \quad \tau_m = 0.985\,\text{Gyr}\,, \\ M_i &\lesssim 2.0\,M_\odot \qquad \text{for} \quad \tau_m = 0.5\,\text{Gyr}\,. \end{aligned} \tag{5}$$

For the shortest timescale ($\tau_m = 0.16\,$Gyr), a considerable extrapolation of our results allows us to estimate that this upper limit to M_i lies between $2.5\,M_\odot$ and $3\,M_\odot$. In § 3.7, we show that the surface lithium abundance allows us to place much tighter limits on the main-sequence mass loss.

3.4. *The Mixing Length*

Table 1 demonstrates that models with larger initial masses M_i require larger mixing length parameters α in order to match the present solar effective temperature; the required increase in α is much larger for long mass loss timescales τ_m than for short ones. For $M_i = 1.8\,M_\odot$ with the longest timescale ($\tau_m = 0.985\,$Gyr), the required α value is double that of the standard solar model. However, for $M_i \leq 1.2\,M_\odot$, the required value of α is only slightly different from that of the standard solar model (i.e., within 10%). If the mass loss timescale is short ($\tau_m = 0.16\,$Gyr), even a large initial mass of $M_i = 1.8\,M_\odot$ requires only a small (10%) increase in α. This behavior is much the same as that of the presolar helium abundance Y, for much the same reason, except that α is determined from matching the solar effective temperature at the solar age.

The mass $M_{ce}^{(\odot)}$ of the convective envelope at the solar age follows the behavior of the mixing length parameter α (see Table 1). It remains at approximately the same value for $M_i \leq 1.2\,M_\odot$ or for $\tau_m = 0.16\,$Gyr. However, for the most extreme case, $M_i = 1.8\,M_\odot$ with $\tau_m = 0.985\,$Gyr, the convective envelope mass at the solar age is more than double that of the standard solar model.

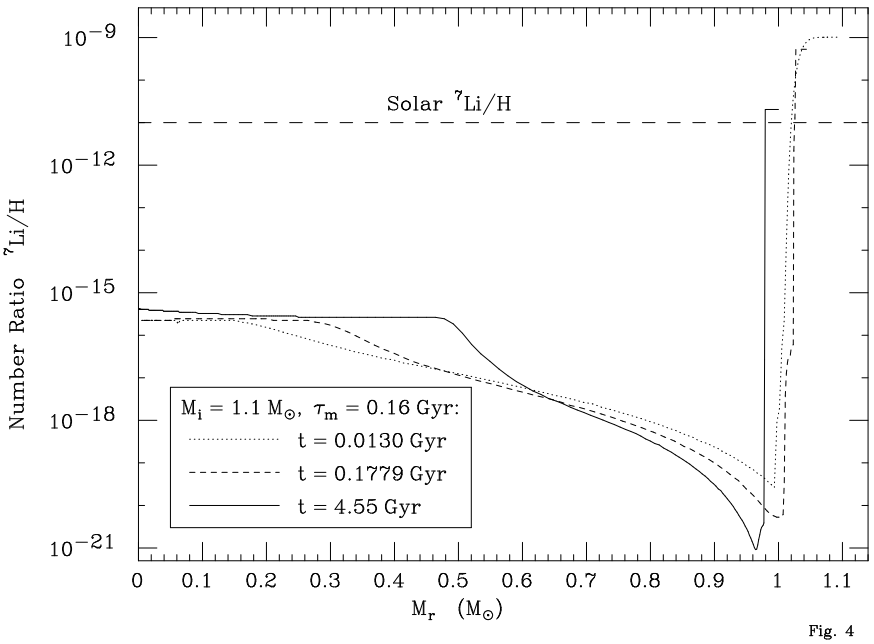

Fig. 4—The profile of the ^{7}Li/H number ratio in the interior of a mass losing solar model at three different times, namely near the ZAMS, partway through the mass loss episode, and at the solar age.

3.5. *The Central Hydrogen Depletion*

The value of the central hydrogen abundance $X_c^{(\odot)}$ at the solar age illustrates the change in the abundance profile which causes the behavior of Y and α described above. Only for the high M_i cases with large τ_m has central hydrogen been depleted much further than for the standard case. For the case $M_i = 1.8\,M_\odot$ with $\tau_m = 0.985$ Gyr, there is only half as much hydrogen left at the center as for the standard case.

3.6. *Solar Neutrinos*

For all mass-losing cases, the predicted ^{37}Cl neutrino capture rate is larger than that for the standard case, although this increase is small for the $M_i = 1.1\,M_\odot$ case (8.5−9.0 SNU's, compared to 8.3 SNU's for the standard case). Note that these neutrino rates were calculated for for $L_\odot = 3.90 \times 10^{33}$ erg/sec; for the more recent value of $L_\odot = 3.86 \times 10^{33}$ erg/sec, these capture rates would be reduced by 0.6 SNU's (see Paper I).

The behavior of the predicted ^{37}Cl neutrino capture rate as a function of M_i and τ_m, as shown in Table 1, is similar to that of the quantities described in the sections above. Predicted capture rates for ^{7}Li, ^{81}Br, and ^{98}Mo targets (47 SNU's, 28 SNU's, and 19 SNU's respectively for the standard case) behave very similarly to the predicted capture rate for ^{37}Cl. However, capture rates for targets such as ^{71}Ga and ^{115}In, which are sensitive primarily to neutrinos from the *p-p* reaction, would barely increase at all. Even for the most extreme case ($M_i = 1.8\,M_\odot$ and $\tau_m = 0.985$ Gyr), the ^{71}Ga and ^{115}In capture rates are increased only by factors of 1.5 and 1.2 respectively over their values for the standard model (which are 130 SNU's and 630 SNU's respectively).

In principle, combining the results of the ^{37}Cl experiment and the ^{71}Ga experiment could help decide whether there has been major mass loss. However, this would require that all neutrinos escape the center of the sun and thus be detectable. The observed low ^{37}Cl capture rate eliminates any hope of resolving between different mass loss cases via neutrino observations. Furthermore, the observed solar lithium abundance precludes an initial solar mass much above 1.1 $M_\odot$, as described in § 3.7 below; thus *none* of the predicted neutrino capture rates would be significantly different from those of the standard model.

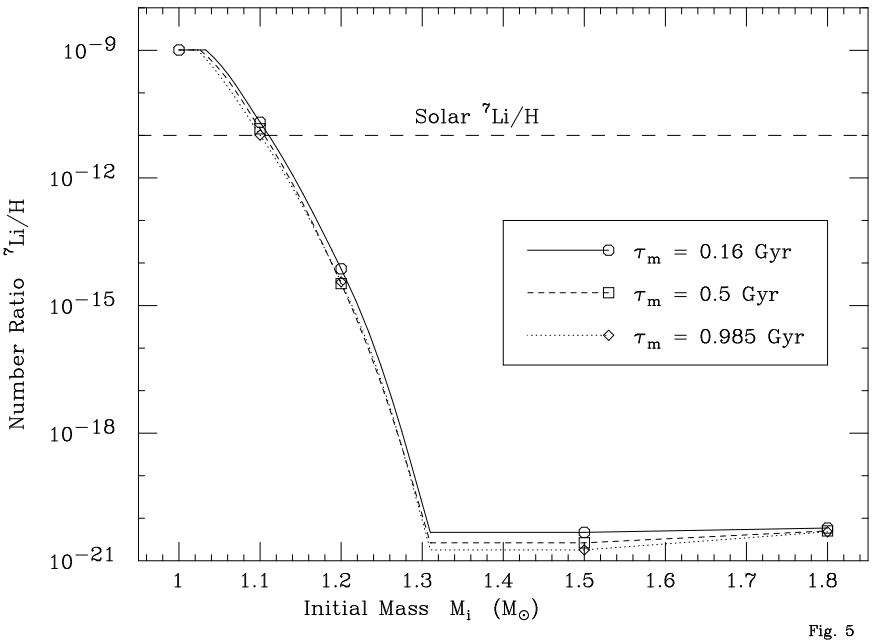

Fig. 5—The predicted surface ^{7}Li abundance for our mass losing solar models for various initial masses and mass loss timescales. (The positions of the breaks in the curves are approximate.)

3.7. *The Case of the Missing Lithium*

3.7.1. Lithium in Detailed Models

We have taken ^{7}Li destruction (and production) into account throughout the interior structure and time evolution of our solar models, using the nuclear reaction rates of Caughlan & Fowler (1988), as described in § 2. Fig. 4 illustrates the profile of ^{7}Li for the case of $M_i = 1.1\ M_\odot$ with $\tau_m = 0.16$ Gyr, at three different times during the main-sequence evolution: near the ZAMS (at $t = 0.013$ Gyr), about half-way through the mass loss phase (at $t = 0.178$ Gyr), and at the solar age (at $t = 4.55$ Gyr). One sees how mass loss eats beyond the steep decline of the lithium profile, and how the convective envelope acts as a reservoir for lithium.

Fig. 5 illustrates one of the key results of this paper, namely, the surface ^{7}Li abundance at the solar age as a function of initial mass M_i and mass loss timescale τ_m. One sees that for a high initial mass ($M_i = 1.8\ M_\odot$, $1.5\ M_\odot$, and even $1.2\ M_\odot$), there is almost *no* ^{7}Li left at the surface; on the other hand, *an initial mass of* $M_i = 1.1\ M_\odot$, *i.e., a mass loss of* $0.1\ M_\odot$, *reproduces almost exactly the observed* ^{7}Li *abundance at the solar surface*, namely a main-sequence depletion by a factor of 100 from a ZAMS value of Li/H = 10^{-9}. (For such models, Proffitt & Michaud [1989] predict a pre–main-sequence ^{7}Li depletion factor of 1.5, for a total depletion factor of 150 from the *presolar* ^{7}Li abundance.) Another key result displayed in Fig. 5 is that *the surface* ^{7}Li *depletion is almost independent of the mass loss timescale* τ_m. To be precise, to match a main-sequence solar ^{7}Li depletion factor of 100 requires mass loss of

$$\begin{aligned} \Delta M &\simeq 0.112\ M_\odot \qquad \text{for} \quad \tau_m = 0.16\ \text{Gyr}\,, \\ \Delta M &\simeq 0.106\ M_\odot \qquad \text{for} \quad \tau_m = 0.5\ \text{Gyr}\,, \\ \Delta M &\simeq 0.100\ M_\odot \qquad \text{for} \quad \tau_m = 0.985\ \text{Gyr}\,. \end{aligned} \tag{6}$$

(These total mass loss values were obtained by taking the $M_i = 1.1\,M_\odot$ cases and using the slope of Fig. 5 to estimate how much further mass loss would be required to obtain a main-sequence depletion factor of 100.) The fact that the ^{7}Li depletion is not a monotonic function of τ_m for the $M_i = 1.2\ M_\odot$ cases (see Fig. 5) *may* be a numerical artifact, due perhaps to the slight inaccuracy of the match to the current sun. However, it may well be a real effect, since

the greatest depth reached by envelope convection switches from being an increasing function of τ_m to a decreasing function of τ_m at this initial mass, and M_{ce} and $M_{\rm Li}$ are also functions of τ_m: one of these working against the other could result in non-monotonic behavior of the ^{7}Li depletion as a function of τ_m.

We have used a number ratio of Li/H $= 1.0 \times 10^{-9}$ for the ZAMS ^{7}Li abundance, corresponding to a presolar value of Li/H $= 1.5 \times 10^{-9}$. An upper limit for the main-sequence mass loss may be obtained by taking the largest reasonable initial ^{7}Li abundance, i.e., a ZAMS ^{7}Li abundance equal to the observed meteoritic value of Li/H $= 2.6 \times 10^{-9}$ (Boesgaard & Steigman 1985). This would shift the steep left portion of the curves in Fig. 5 upward by a factor of 2.6, and would imply a somewhat larger mass loss of

$$\begin{aligned} \Delta M &\simeq 0.128\, M_\odot \qquad \text{for} \quad \tau_m = 0.16\,\text{Gyr}\,, \\ \Delta M &\simeq 0.122\, M_\odot \qquad \text{for} \quad \tau_m = 0.5\,\text{Gyr}\,, \\ \Delta M &\simeq 0.116\, M_\odot \qquad \text{for} \quad \tau_m = 0.985\,\text{Gyr}\,. \end{aligned} \tag{7}$$

Note that Guzik *et al.* (1987) concluded that a solar model with $M_i = 2\, M_\odot$ would result in total surface ^{7}Li (and ^{9}Be) depletion; they did not use this to attempt to place limits on main-sequence mass loss, but instead suggested that the observed solar abundances of ^{7}Li and ^{9}Be could perhaps be achieved via spallation reactions in solar flares. Schramm, Steigman, & Dearborn (1990) point out two strong arguments against this production mechanism. First, spallation reactions would badly underproduce ^{7}Li relative to ^{9}Be. (The problem of spallation overproduction of ^{6}Li relative to ^{7}Li could possibly be avoided by ^{6}Li burning at the base of the convective envelope, but neither ^{7}Li nor ^{9}Be abundances would be affected: the convective envelope does not reach down to high enough temperatures to burn either of these.) Second, the energy available for spallation in solar flares is totally insufficient to produce the required amount of ^{7}Li, provided that the present rate of flare activity was typical of the sun's past also. Guzik *et al.* (1987) argue that observations of X-ray fluxes of F- and G-type stars of ages younger than ~ 1.0 Gyr show that in such stars there *would* be enough energy to produce the necessary amount of ^{7}Li and ^{9}Be over a timescale of ~ 1.0 Gyr (note that these stars would resemble the early sun, for a mass-losing case). In any case, the first objection remains: the observed solar ^{7}Li/^{9}Be ratio is far from what one would expect from spallation reactions.

3.7.2. The Lithium Depletion–Mass Loss Formula

Using the same approach as Weymann & Sears (1965), Hobbs *et al.* (1989) presented a formula for the amount of mass loss, ΔM, required to match any observed lithium depletion $f \equiv {\rm Li}_f/{\rm Li}_i$, namely

$$\Delta M = (M_{\rm Li} - M_{ce}) - M_{ce} \ln f\,, \tag{8}$$

where M_{ce} is the mass of the convective envelope and $M_{\rm Li}$ is the depth in mass below the initial mass surface at which lithium is burned. Note that the above formula assumes that the convective envelope mass M_{ce} remains constant while the mass loss is taking place, and that the lithium discontinuity at $M_{\rm Li}$ is sharp; the depletion factor f is that of *main-sequence* ^{7}Li depletion. The simplest approach is to use values obtained from a standard solar model at the solar age. From Table 1, our standard solar model at the solar age has a convective envelope mass of $M_{ce}^{(\odot)} = 0.017\, M_\odot$, and lithium has burned to half its initial abundance at a depth $M_{\rm Li}^{(1/2)} = 0.029\, M_\odot$; for a lithium depletion $f = 1/100$, eq. (8) would then yield a mass loss of $\Delta M = 0.090\, M_\odot$. This is in fairly good agreement with the results (shown in eq. [6]) of our detailed calculations. Use of the values from Table 1 for the cases $M_i = 1.1\, M_\odot$, namely $M_{\rm Li}^{(1/2)} \approx 0.05\, M_\odot$ and $M_{ce} \approx 0.019\, M_\odot$, results in a value of $\Delta M \approx 0.118\, M_\odot$, nearly as far off in the other direction. Using eq. (8), Hobbs *et al.* (1989) obtained a mass loss $\Delta M = 0.041\, M_\odot$: this resulted from their use of an older solar model (Iben 1967), which had a much smaller convective envelope mass (of $M_{ce}^{(\odot)} = 0.0045\, M_\odot$) than is obtained by most authors for recent solar models (see Paper I). They also have a smaller value of $M_{\rm Li} = 0.025\, M_\odot$ than our value of $0.029\, M_\odot$. The former value was obtained by Hobbs *et al.* (1989)

by taking the commonly used value for lithium burning of $T \approx 2.5 \times 10^6\ K$: at this temperature, the ^{7}Li burning timescale is 7 Gyr, so that about half of the initial lithium would be burned after 4.55 Gyr. Thus for the standard solar model, the definition of $M_{\rm Li}$ used by Hobbs *et al.* (1989) is the same as our definition, and the slight difference between their value of $0.025\ M_\odot$ and ours of $0.029\ M_\odot$ is due to a difference in the structure of the two solar models.

From Table 1, one can check the assumption made in eq. (8) that the convective envelope mass M_{ce} remains constant from the moment when the convective envelope reaches the lithium discontinuity to the moment mass loss terminates. The quantity $M_{ce}^{\rm Li}$ is the mass of the convective envelope at the moment when surface lithium has declined by a factor of two, i.e., shortly after the convective envelope encountered the lithium discontinuity. The quantity $M_{ce}^{\rm max}$ is the mass of the convective envelope at its maximum extent, which occurs at the moment that mass loss terminates. The difference between these shows the extent to which the convective envelope mass deviates from constancy. For the $M_i = 1.1\ M_\odot$ cases, this deviation from constancy is about $0.005\ M_\odot$, which is about a quarter of the convective envelope mass. For a depletion $f = 1/100$, a change of this size in the value used for M_{ce} would result in a change of nearly 20% in the mass loss predicted by eq. (8). The situation grows rapidly worse for larger amounts of mass loss: the mass of the convective envelope changes by a factor of three for the $M_i = 1.2\ M_\odot$ cases.

Swenson (1990) has noted that eq. (8) has limited validity; in a forthcoming paper, he and Faulkner intend to discuss its drawbacks and possible improvements. It is clear that eq. (8) will work less well for stars either more massive or less massive than the sun, even if the most appropriate values of M_{ce} and $M_{\rm Li}$ are used (rather than the solar values, which could be rather poor approximations). For stars more massive than the sun, the convective envelope mass declines increasingly quickly as a function of stellar mass, and the assumption that M_{ce} is constant during mass loss is violated. For stars less massive than the sun, the large observed amount of ^{7}Li depletion requires relatively large amounts of mass loss, with the same result that M_{ce} is not constant; in addition, pre–main-sequence ^{7}Li depletion can be significant for such stars.

Recently, Swenson & Faulkner (1990) computed some stellar models with main-sequence mass loss, evolving them to an age of 0.6 Gyr (the age of the Hyades). Their models indicated that, if main-sequence mass loss was assumed to be the cause of the observed Hyades ^{7}Li depletion, then most Hyades G dwarfs must descend from an extremely small range of initial masses (e.g., $1.08 \pm 0.01\ M_\odot$), with the different ^{7}Li abundances and effective temperatures being due to different mass loss rates; and any stars with lower initial masses would have to suffer sufficient mass loss to deplete ^{7}Li below the observable threshold, while higher initial masses encountered very little mass loss. Such a sharp-edged (nearly step-function) distribution of mass loss rates as a function of initial stellar mass seems improbable, suggesting that main-sequence mass loss is unlikely to be the explanation for main-sequence ^{7}Li depletion.

3.7.3. The Lithium-Burning Temperatures

Figs. 6*a* and *b* show the temperature history of the deepest mass layer ever reached by envelope convection, for our shortest and longest mass loss timescales. For the constant-mass $1.0\ M_\odot$ case, the deepest convective envelope occurs at the beginning of the main-sequence evolution, and retreats thereafter. The temperature for that *mass layer* is shown in Figs. 6*a* and *b*: it remains very nearly constant at $2.5 \times 10^6\ K$. Lithium *at this layer* is depleted by a factor of 1/2 at the solar age, but even if the convective envelope had not quickly retreated from this layer, there still would not have been any significant surface lithium depletion, since the mass of the burning layer is much smaller than the mass of the convective envelope. (Note that, in fact, the convective envelope has retreated to a temperature of $2 \times 10^6\ K$ by the solar age.)

Figs. 6*a* and *b* show that the convective envelope for the $M_i = 1.1\ M_\odot$ cases reaches down to layers that have experienced temperatures of $4 \times 10^6\ K$, and that the temperature at this layer declines with a timescale τ_T, which is two to three times as long as the mass loss timescale τ_m. (Note that τ_T is *not* the same for all layers of the star.) More relevant to the surface lithium depletion is the behavior which determines the position of the lithium discontinuity. For the $M_i = 1.1\ M_\odot$ cases, and for the $M_i = 1.2\ M_\odot$ case with the long mass loss timescale, Figs. 6*a*

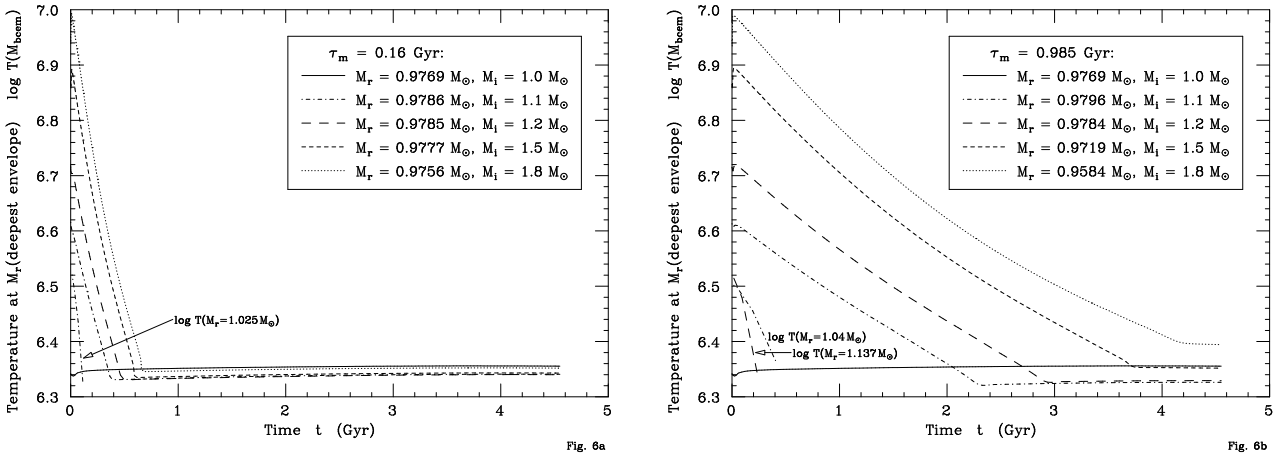

Fig. 6—Temperature as a function of time for the deepest mass layer in the star ever reached by surface convection. For some models, the temperature as a function of time for a mass layer near the lithium discontinuity is also given (see text).

and *b* show the behavior of the temperature for the mass layers at which burning reduces the lithium abundance by a factor of 100. For the $M_i = 1.1\,M_\odot$, $\tau_m = 0.16\,\mathrm{Gyr}$ case (see Fig. 6*a*), this mass layer is at $M_r = 1.025\,M_\odot$, i.e., at a depth of $M_{\rm Li}^{(1/100)} = 0.075\,M_\odot$ below the initial surface. (Note that this is somewhat deeper than $M_{\rm Li}^{(1/2)} = 0.061$ for this case: this illustrates the fact that the lithium discontinuity is *not* sharp, but spread out over a mass range comparable to the mass of the convective envelope. This is another source of error in the mass loss formula of eq. [8].) Similarly, for the $M_i = 1.1\,M_\odot$, $\tau_m = 0.985\,\mathrm{Gyr}$ case, the temperature behavior is shown in Fig. 6*b* for the mass layer $M_r = 1.04\,M_\odot$, i.e., $M_{\rm Li}^{(1/100)} = 0.06\,M_\odot$ (cf. $M_{\rm Li}^{(1/2)} = 0.049\,M_\odot$ from Table 1). For the $M_i = 1.2\,M_\odot$, $\tau_m = 0.985\,\mathrm{Gyr}$ case, the temperature is shown for $M_r = 1.137\,M_\odot$, i.e., $M_{\rm Li}^{(1/100)} = 0.063\,M_\odot$ (cf. $M_{\rm Li}^{(1/2)} = 0.052\,M_\odot$ from Table 1). (Again, these illustrate the spread in the lithium profile.) From Figs. 6*a* and *b*, one can see that the initial temperatures of these layers near the bottom of the lithium discontinuity lay between $3.2 \times 10^6\,K$ and $3.3 \times 10^6\,K$. The corresponding initial temperatures for the $M_{\rm Li}^{(1/2)}$ layers lay between $2.95 \times 10^6\,K$ and $3.05 \times 10^6\,K$; for the purposes of eq. (8), $M_{\rm Li}^{(1/2)}$ gives a better estimate of the position of the lithium "discontinuity". In other words, *for mass-losing cases, the initial temperature at the mass layer of the lithium discontinuity is not* $2.5 \times 10^6\,K$ (as would be commonly assumed), *but rather* $3 \times 10^6\,K$. Recall, as noted above, that for the constant-mass case the corresponding temperature *is* indeed $2.5 \times 10^6\,K$. The difference lies in the fact that for the constant-mass case the temperature at this layer remains practically constant with time, while for the mass losing cases the temperature drops fairly steeply with time. The appropriate initial temperature for lithium burning can be derived analytically, assuming a knowledge of τ_T.

Assuming that the temperature at a given layer drops exponentially, i.e., $T = T_i \exp(-t/\tau_T)$, and that the nuclear burning rate is proportional to T^ν, then the abundance X of an element at this layer drops as

$$\frac{dX}{dt} = -\frac{X}{\tau_{\rm nuc}(T)} = -\frac{X}{\tau_{\rm nuc}(T_i)}\left(\frac{T}{T_i}\right)^\nu = -\frac{X}{\tau_{\rm nuc}(T_i)} e^{-\nu t/\tau_T}\,, \tag{9}$$

where $\tau_{\rm nuc}(T)$ is the nuclear burning timescale at temperature T. This equation can be solved to yield X as a function of time t:

$$\begin{aligned} X &= X_i \exp\left[\left(\frac{1}{\tau_{\rm nuc}(T_i)}\frac{\tau_T}{\nu}\right)\left(e^{-\nu t/\tau_T} - 1\right)\right]\,, \\ \text{i.e.,}\quad X_f &= X_i \exp\left[-\left(\frac{1}{\tau_{\rm nuc}(T_i)}\frac{\tau_T}{\nu}\right)\right] \quad \text{for} \quad t \gg \frac{\tau_T}{\nu}\,. \end{aligned} \tag{10}$$

The timescale τ_T with which the temperature drops depends on the initial mass and the mass loss rate; it is also not constant throughout the stellar interior. Looking at the appropriate layers (i.e., at $M_{\rm Li}^{(1/2)}$) in our detailed models, we can estimate that for initial masses not too far from 1.0 $M_\odot$ the timescale τ_T for layers relevant to the lithium discontinuity is

$$\tau_T \sim -\frac{1}{5}\left(\frac{M_i}{\dot{M}_i}\right) \approx \frac{\tau_m M_i}{5(M_i - M_f)}\,, \tag{11}$$

where eq. (2) has been used to give an expression for the initial mass loss rate $\dot{M}_i$. Using this empirical relation for τ_T and the depletion given by eq. (10), one may estimate the *initial* nuclear burning timescale required to obtain a given depletion $f = X_f/X_i$ in a mass losing model:

$$\tau_{\rm nuc}(T_i) = -\frac{\tau_T}{\nu \ln f} \sim \frac{1}{5\nu \ln f}\left(\frac{M_i}{\dot{M}_i}\right) \approx -\frac{\tau_m M_i}{5\nu(M_i - M_f)\ln f}\,. \tag{12}$$

For lithium burning, the nuclear timescale $\tau_{\rm nuc}$ for several temperatures is given in Table 2, along with the corresponding values of the nuclear power index ν and the timescale τ_T for a depletion $f = 1/2$. For the $M_i = 1.1 M_\odot$, $\tau_m = 0.985$ Gyr case, $M_i/|\dot{M}_i| = 9.85$ Gyr, implying $\tau_T \sim 2$ Gyr; looking in Table 2, this would imply an initial temperature of $\sim 2.95 \times 10^6\,K$ for the lithium burning layer. This is precisely the value obtained from our detailed model. However, this formula does not always provide such a perfect estimate: for the $M_i = 1.1\,M_\odot$, $\tau_m = 0.16$ Gyr case, the formula gives an initial temperature of $\sim 3.2 \times 10^6\,K$, as compared to the value from our detailed models of $3.06 \times 10^6\,K$. Part of this discrepancy for the short timescale comes from the pre–main-sequence evolution of our models, a period of order 10 million years during which the temperature at the lithium-burning layer is approximately constant at its initial ZAMS value. In effect, the timescale τ_T for the temperature decline is longer initially; the speed of the decline increases later.

Note that for constant-mass models a depletion f requires a nuclear burning timescale $\tau_{\rm nuc} = -t_\odot/\ln f$. For a depletion factor of $f = 1/2$, this implies $\tau_{\rm nuc} = 6.6$ Gyr; from Table 2, this yields a lithium burning temperature of $2.5 \times 10^6\,K$, which implies $M_{\rm Li}^{(1/2)} = 0.029\,M_\odot$.

3.7.4. Beryllium Depletion

One can use the same approach to determine the initial temperature for ^{9}Be burning. Table 3 gives the corresponding values. For the $M_i = 1.1\,M_\odot$ case with the long mass loss timescale ($\tau_m = 0.985$ Gyr), the temperature is estimated to be $\sim 3.81 \times 10^6 K$, while for the $M_i = 1.1\,M_\odot$ case with the short mass loss timescale ($\tau_m = 0.16$ Gyr), the temperature is estimated to be $\sim 4.09 \times 10^6\,K$; from our models, these would imply masses $M_{\rm Be}^{(1/2)} = 0.102\,M_\odot$ and $0.131\,M_\odot$, respectively. The mass loss necessary to match the observed solar lithium abundance was $\Delta M = 0.100\,M_\odot$ and $0.112\,M_\odot$, respectively (see eq. [6]: these values were obtained using ZAMS ^{7}Li/H $= 1.0 \times 10^{-9}$). (The slightly larger initial mass of $M_i = 1.112\,M_\odot$ for the short timescale case would would presumably result in a correspondingly slightly larger mass of $M_{\rm Be}^{(1/2)} = 0.132\,M_\odot$.) The convective envelope reaches further downwards by an additional $0.020\,M_\odot$ and $0.022\,M_\odot$, for the long and the short timescales, respectively (see Table 1). It thus reaches layers $0.120\,M_\odot$ and $0.134\,M_\odot$, respectively, beneath the original surface. Thus some beryllium-depleted material would be mixed to the surface, but not much: inverting eq. (8) for the case of ^{9}Be, one obtains depletion factors of $f = 0.4$ and 0.9, respectively. Considering the errors in our estimates of $M_{\rm Be}^{(1/2)}$, and the slight inaccuracy of eq. (8), this modest depletion is not inconsistent with the observations of the solar beryllium abundance, which shows little or no depletion compared to the cosmic abundance: Boesgaard (1976) gives solar ^{9}Be/H $= 1.13 \times 10^{-11}$, and estimates the cosmic abundance to be ^{9}Be/H $= (1.31 \pm 0.36) \times 10^{-11}$, i.e., $0.7 \lesssim f \lesssim 1$.

If one uses the meteoritic value for the ZAMS lithium abundance, i.e., ^{7}Li/H $= 2.6 \times 10^{-9}$, then one requires a mass loss $\Delta M = 0.116\,M_\odot$ and $0.128\,M_\odot$ for the long and the short mass loss timescales, respectively (see eq. [7]). Using the same method as above, these yield ^{9}Be burning temperatures of $\sim 3.83 \times 10^6\,K$ and $\sim 4.11 \times 10^6\,K$, respectively; from our detailed models, these imply values for $M_{\rm Be}^{(1/2)}$ of about $0.104\,M_\odot$ and $0.139\,M_\odot$, respectively.

We invert eq. (8) to get beryllium depletions of $f = 0.2$ and 0.6, respectively. This agrees with the observed solar ^{9}Be depletion of $f \approx 0.5$, when one uses the meteoritic abundance of $^9\mathrm{Be/H} = 2.5 \times 10^{-11}$ (Cameron 1973) for the presolar value.

We are in the process of modifying our stellar evolution program to include ^{6}Li, ^{9}Be, ^{10}B, and ^{11}B, (and also to allow initial models on the Hayashi track, rather than near the main sequence). A preliminary "nearly solar" test run with $M_i = 1.1\ M_\odot$ and mass loss timescale $\tau_m = 0.5$ Gyr resulted in main-sequence ^{7}Li depletion by a factor $f = 1/125$ and ^{9}Be depletion by a factor $f = 0.32$; comparing to the models of the present paper, we see that the depletion would have been slightly less (slightly higher values of f) if the model had been more accurately matched to the present sun. This preliminary ^{9}Be depletion result agrees fairly well with the above estimates.

For a constant-mass case, one requires a nuclear burning timescale of $\tau_{\rm nuc} = -t_\odot / \ln f$ to get a depletion f at the solar age; for a depletion $f = 1/2$, this implies $\tau_{\rm nuc} = 6.6$ Gyr. Table 3 then yields a ^{9}Be burning temperature of slightly below $3.3 \times 10^6\ K$, giving $M_{\rm Be}^{(1/2)} = 0.065\ M_\odot$. (Note that Hobbs *et al.* [1989] used a temperature of $3.7 \times 10^6\ K$ for ^{9}Be burning, and estimated $M_{\rm Be}^{(1/2)} = 0.07\ M_\odot$.)

4. CONCLUSIONS

1. Early–main-sequence mass loss can solve the case of the missing solar lithium. The mass loss is $0.10 - 0.11 M_\odot$ if one takes the ZAMS ^{7}Li/H ratio to be 1.0×10^{-9}, the maximum value observed in Pop I main-sequence stars. The mass loss is $0.12 - 0.13\ M_\odot$ if one takes the ZAMS ^{7}Li/H ratio to be 2.6×10^{-9}, the meteoritic value. (These mass loss values presume that there is no other mechanism for surface lithium depletion, and thus can be considered to be upper limits. Note that recent work by Swenson & Faulkner [1990] argues against this mass-loss mechanism being primarily responsible for main-sequence lithium depletion.) Note that for initial masses $M_i \sim 1.1\ M_\odot$, standard models show pre–main-sequence ^{7}Li depletion (on the Hayshi track) of a factor of about 1.5 (Proffitt & Michaud 1989): the ZAMS ^{7}Li abundance will have been reduced by this factor from its presolar (interstellar medium) value.

2. The required amount of mass loss is nearly independent of the mass loss timescale.

3. A simple formula (Hobbs *et al.* [1989]: see eq. [8]) exists to estimate the amount of mass loss ΔM required by an observed lithium (or beryllium) depletion f, namely $\Delta M = (M_{\rm Li} - M_{ce}) - M_{ce} \ln f$, where M_{ce} is the convective envelope mass and $M_{\rm Li}$ is the depth in mass (below the initial mass surface) at which lithium (or beryllium) is burned. This mass loss formula works fairly well for stars very close to $1\ M_\odot$ which do not lose much mass (i.e., $\lesssim 0.1\ M_\odot$), *provided* that one obtains good values for M_{ce} and $M_{\rm Li}$. It is expected to be less accurate for stars of higher or lower mass.

4. Constant-mass models burn lithium and beryllium at temperatures of $2.5 \times 10^6 K$ and $3.3 \times 10^6 K$, respectively. In mass losing models, where temperatures decline while the mass loss takes place, higher initial temperatures are required. We have developed a prescription to estimate these temperatures as a function of initial stellar mass M_i and initial mass loss rate $\dot{M}_i$. Instead of requiring $\tau_{\rm nuc} = -t / \ln f$ to get a depletion factor f at age t (as is the case for the constant-mass case), we show that the initial burning timescale has to be shorter, in order to compensate for the temperature decline, namely $\tau_{\rm nuc} = -\tau_T / (\nu \ln f)$, where ν is the nuclear index (i.e., $\tau_{\rm nuc} \propto T^{-\nu}$) and τ_T is the timescale of the temperature decline. (Note that $\nu \sim 20$ for both ^{7}Li burning and ^{9}Be burning.) From our detailed models, we have estimated an empirical formula for τ_T, namely $\tau_T \sim -0.2 (M_i / \dot{M}_i)$. This results in initial temperatures of approximately $3 \times 10^6\ K$ for lithium burning and approximately $4 \times 10^6\ K$ for beryllium burning for the mass-losing cases. (Note that the precise values of these temperatures depend on the initial mass and initial mass loss rate.)

5. Mass losing solar models require smaller values for the presolar helium abundance Y than the standard model, and larger values for the solar metallicity Z, the mixing length parameter α, and the predicted solar neutrino

flux. These differences, however, are negligible if one has a mass loss $\Delta M \sim 0.1\ M_\odot$, which is the value required to match the observed solar lithium depletion.

6. The requirement that the presolar helium abundance be larger than the primordial helium abundance places much less stringent limits on the mass loss than does the lithium depletion. The mass loss ΔM must be less than $0.7\ M_\odot$, $1.0\ M_\odot$, and $1.5 - 2\ M_\odot$ for mass loss timescales of $\tau_m = 0.985$ Gyr, 0.5 Gyr, and 0.16 Gyr respectively.

7. The luminosity history of our mass losing cases is quite different from that of the standard case, first declining during the period of mass loss, and then following the same steady increase as the standard case. The mass losing cases have a higher initial luminosity (by as much as a factor of 15 for the extreme $M_i = 1.8\ M_\odot$ case). However, for our preferred $M_i = 1.1\ M_\odot$ cases, the initial luminosity is only a factor of 1.5 higher than that of the standard case (barely higher than the present solar luminosity), and the total variation in the luminosity is *less* than for the standard case. This different luminosity history, the stronger initial gravitational attraction, and the larger solar wind ($\dot{M} \sim 10^{-10}\ M_\odot$/yr rather than the present rate of $\dot{M} \sim 10^{-14}\ M_\odot$/yr), could have had significant consequences on the planetary system, that should be explored further.

We wish to thank Dr. Steven E. Koonin for the support supplied by the Kellogg Radiation Laboratory. One of us (A. I. B.) wishes in addition to thank Drs. Scott D. Tremaine and Peter G. Martin for the support provided by the Canadian Institute for Theoretical Astrophysics.

We are indebted to Dr. Charles A. Barnes for encouragement and enlightening discussions, and to Fritz J. Swenson (the referee) for helpful comments and information.

One of us (I.-J. S.) wishes to express her gratitude to Dr. Robert F. Christy, her husband, for his generosity in help, be it with insightful discussions or with tasks of daily life. She is also indebted to the irreplaceable support of Mrs. Lilly Stelter, her mother, who drove thousands of miles many a time to assist with the care of children so that the research could be more effectively pursued.

We wish to acknowledge the work of Kathleen E. Kraemer, who as a Caltech summer student in 1988 carried out many computations with an earlier version of the stellar evolution program.

This work was supported in part by a grant from the National Science Foundation PHY-8817296.

This work was supported in part by a grant from the Natural Sciences and Engineering Research Council of Canada.

REFERENCES

Allen, C. W. 1963, *Astrophysical Quantities*, 2nd ed. (London: Athlone Press), p. 17

Bahcall, J. N., Huebner, W. F., Lubow, S. H., Parker, P. D., and Ulrich, R. K. 1982, Rev. Mod. Phys., 54, 767

Bahcall, J. N., and Ulrich, R. K. 1988, Rev. Mod. Phys., 60, 297

Bodenheimer, P. 1965, ApJ, 142, 451

Boesgaard, A. M., and Steigman, G. 1985, ARA&A, 23, 319

Boesgaard, A. M. 1976, ApJ, 210, 466

Boothroyd, A. I., and Sackmann, I.-J. 1988, ApJ, 328, 653

Brown, A., Vealé, A., Judge, P., Bookbinder, J., and Hubeny, I. 1990, in *Cool Stars, Stellar Systems, and the Sun: 6th Cambridge Workshop, Astronomical Society of the Pacific Conference Series*, Vol **9**, ed. G. Wallerstein (San Francisco: Bookcrafters), p. 183

Cameron, A. G. W. 1973, Space Sci. Rev., 15, 121

Caughlan, G. R., and Fowler, W. A. 1988, At. Data Nucl. Data Tables, 40, 283

Cayrel, R., Cayrel de Stobel, G., Campbell, B., and Däppen, W. 1984, ApJ, 283, 205

Cox, A. N, and Stewart, J. N. 1970, ApJS, 19, 243

D'Antona, F., and Mazzitelli, I. 1984, A&A, 138, 431

Dominy, J. F., and Wallerstein, G. 1987, ApJ, 317, 810

Dominy, J. F., Wallerstein, G., and Suntzeff, N. B. 1986, ApJ, 300, 325

Duncan, D. K., and Jones, B. F. 1983, ApJ, 271, 663

Grevesse, N. 1984, Physica Scripta, T8, 49

Guenther, D. B., Jaffe, A., and Demarque, P. 1989, ApJ, 345, 1022

Guzik, J. A., Willson, L. A., and Brunish, W. M. 1987, ApJ, 319, 957

Hobbs, L. M., Iben, I., Jr., and Pilachowski, C. 1989, ApJ, 347, 817

Hobbs, L. M., and Pilachowski, C. 1988, ApJ, 334, 734

Keady, J. 1985, private communication

Kızıloğlu, N., and Eryurt-Ezer, D. 1985, A&A, 146, 384

Proffitt, C. R., and Michaud, G. 1989, ApJ, 346, 976

Sackmann, I.-J., Boothroyd, A. I., and Fowler, W. A. 1990, ApJ, 360, 727

Schramm, D. N., Steigman, G., and Dearborn, D. S. P. 1990, preprint FERMILAB-Pub-90/13-A

Swenson, F. J. 1990, private communication

Swenson, F. J., and Faulkner, J. 1990, BAAS, 21, 1101

Swenson, F. J., Stringfellow, G. S., and Faulkner, J. 1990, ApJ (Letters), 348, L33

Weymann, R., and Sears, R. L. 1965, ApJ, 142, 174

Willson, L. A., and Bowen, G. H. 1984, Nature, 312, 429

Willson, L. A., Bowen, G. H., and Struck-Marcell, C. 1987, Comm. Ap., 12, 17

Willson, L. A., Guzik, J. A., and Brunish, W. M. 1986, preprint

Table 1

Characteristics of Standard and Mass-Losing Solar Models [a]

M_i ($M_\odot$)	τ_m (Gyr)	Y	Z	α	$X_c^{(\odot)}$	$\nu(^{37}\mathrm{Cl})$ (SNU)	$\left[\frac{\mathrm{Li}}{\mathrm{H}}\right]^{(\odot)}$	$M_{ce}^{(\odot)}$ ($M_\odot$)	$M_{ce}^{\max}$ ($M_\odot$)	M_{ce}^{Li} ($M_\odot$)	$M_{\mathrm{Li}}^{(1/2)}$ ($M_\odot$)
1.0	—	0.2793	0.01940	2.36	0.3593	8.26	1.02-9[b]	0.0170	0.0231	—	0.029[c]
1.1	0.16	0.2788	0.01942	2.38	0.3570	8.52	2.04-11	0.0173	0.0224	0.0171	0.061
1.1	0.5	0.2776	0.01945	2.40	0.3515	8.78	1.43-11	0.0177	0.0219	0.0166	0.053
1.1	0.985	0.2759	0.01949	2.44	0.3438	8.96	1.02-11	0.0185	0.0204	0.0166	0.049
1.2	0.16	0.2779	0.01944	2.39	0.3541	8.68	7.30-15	0.0176	0.0215	0.0087	0.065
1.2	0.5	0.2749	0.01952	2.47	0.3421	9.16	3.28-15	0.0189	0.0216	0.0086	
1.2	0.985	0.2712	0.01962	2.55	0.3237	10.3	3.60-15	0.0203	0.0216	0.0092	0.052
1.5	0.16	0.2747	0.1952	2.45	0.3414	9.12	4.66-21	0.0187	0.0223	3.0-5[b]	
1.5	0.5	0.2649	0.01979	2.71	0.3050	12.0	2.64-21	0.0229	0.0249	6.5-5	
1.5	0.985	0.2519	0.02014	2.98	0.2553	15.1	1.80-21	0.0278	0.0281	2.5-4	
1.8	0.16	0.2693	0.01967	2.60	0.3286	10.5	5.87-21	0.0211	0.0244	3.-9	
1.8	0.5	0.2496	0.02020	3.11	0.2650	16.4	5.03-21	0.0293	0.0304	4.-9	
1.8	0.985	0.2244	0.02088	4.10	0.1806	23.0	4.79-21	0.0416	0.0416	1.3-6	

[a] Note: a superscript "$(\odot)$" indicates a value at the solar age; $M_{ce}^{\max}$ is the maximum convective envelope mass during the evolution (occurring just when mass loss terminates); M_{ce}^{Li} is the convective envelope mass at the time when the surface ^{7}Li abundance has dropped by a factor of two, i.e., soon after the base of the convective envelope encounters ^{7}Li-depleted layers; $M_{\mathrm{Li}}^{(1/2)}$ is the depth in mass below the original surface at which burning has reduced ^{7}Li to half its original abundance.

[b] Power of ten notation: $1.02\text{-}9 \equiv 1.02 \times 10^{-9}$, etc.

[c] At the solar age.

Table 2

^{7}Li Burning Timescales for Appropriate Temperatures and Densities [a]

T (10^6 K)	ρ (g/cm^3)	reaction rate (cm^3/mole-sec)	$\tau_{\rm nuc}$ (Gyr)	nuclear index ν	expected τ_T (Gyr)
2.5	0.245	2.67×10^{-17}	6.9	20.2	97.
2.6	0.279	5.85×10^{-17}	2.78	19.9	38.
2.7	0.317	1.23×10^{-16}	1.16	19.6	15.8
2.8	0.360	2.51×10^{-16}	0.50	19.4	6.7
2.9	0.410	4.93×10^{-16}	0.224	19.2	3.0
3.0	0.465	9.41×10^{-16}	0.103	18.9	1.36
3.1	0.528	1.74×10^{-15}	0.049	18.7	0.64
3.2	0.597	3.15×10^{-15}	0.0241	18.5	0.31
3.3	0.673	5.55×10^{-15}	0.0121	18.3	0.154
3.4	0.758	9.57×10^{-15}	0.0062	18.1	0.078
3.5	0.853	1.62×10^{-14}	0.0033	17.9	0.041

[a] Note: the nuclear timescale is computed for a hydrogen abundance $X = 0.7$ by mass and the given densities ρ, which should be within 10% of the correct values for ZAMS models with initial masses $0.9\ M_\odot \lesssim M_i \lesssim 1.2\ M_\odot$; the expected τ_T values are for a ^{7}Li depletion of $f = 1/2$.

Table 3

^{9}Be Burning Timescales for Appropriate Temperatures and Densities [a]

T (10^6 K)	ρ (g/cm^3)	reaction rate (cm^3/mole-sec)	$\tau_{\rm nuc}$ (Gyr)	index ν	expected τ_T (Gyr)
3.3	0.673	1.19×10^{-17}	5.6	22.5	88.
3.4	0.758	2.33×10^{-17}	2.57	22.3	40.
3.5	0.853	4.43×10^{-17}	1.20	22.1	18.4
3.6	0.957	8.23×10^{-17}	0.57	21.8	8.7
3.7	1.07	1.49×10^{-16}	0.28	21.7	4.3
3.8	1.19	2.66×10^{-16}	0.143	21.5	2.13
3.9	1.33	4.63×10^{-16}	0.074	21.3	1.09
4.0	1.47	7.92×10^{-16}	0.039	21.0	0.57
4.1	1.63	1.33×10^{-15}	0.0208	20.8	0.30
4.2	1.80	2.20×10^{-15}	0.0114	20.6	0.163
4.3	1.97	3.58×10^{-15}	0.0064	20.4	0.091
4.4	2.20	5.73×10^{-15}	0.0036	20.3	0.050
4.5	2.39	9.06×10^{-15}	0.0021	20.1	0.029

[a] See note for Table 2.